Spatial Localization of Greenland Mass Wasting Using a 2-D Wavelet Decomposition of GRACE Data and Comparison to Physical Drivers of Ice Loss

Benjamin Getraer

Senior Thesis Draft

Presented to the Faculty

of Princeton University

in Candidacy for the Degree

of Bachelor of Arts

Recommended for Acceptance

by the Department of

Geosciences

Adviser: Laure Resplandy

Second Reader: Frederik J. Simons

April 15, 2019

This paper represents my own work in accordance with University regulations,

Benjamin Getraer

Abstract

Melting ice from the Greenland Ice-Sheet has accounted for an increasing percentage — now estimated at 25% — of rising global mean sea-level since the early 1990s. As recently as 2016, gravimetric and altimetric studies of Greenland melting rates found increasing rates of ice loss, which have not been borne out in GRACE gravimetric observations over the last few years (2015–2017). We hypothesize that the true trend of Greenland ice loss between 2003–2017 is linear, and that deviations from the linear trend may be explained by inter-annual variability in climate. We demonstrate a novel application of 2-dimensional discrete wavelet analysis to the GRACE dataset to recover spatial structure of inter-annual variability in ice loss, focusing on the unusual melt and accumulation seasons of 2012–2014. Finally, we compare our interpretation of the 2012–2014 anomaly in spatial scale and location to the results of others using independent atmospheric, altimetric, and meteorologic data sources.

Key Points:

1. We focus on inter-annual variability of the Greenland ice loss trend.
2. We analyze subregional signals using discrete wavelet transforms.
3. We define the 2012–2014 anomaly in spatial structure.

Acknowledgements

Thank you to my thesis adviser Prof. Laure Resplandy who has helped me think through my research questions, understand atmospheric processes, and for her support and patience in helping me with the direction this project has taken. Thank you to my Junior Paper adviser and second reader Prof. Frederik J. Simons who helped me with the conceptualization, direction, and revision of earlier portions of this project. Frederik's excitement about research and support of undergrads trying to wrap their heads around complex ideas has been a major reason why I chose to concentrate in Geosciences. Thank you to the second reader of my Fall Junior Paper, Prof. Jessica Irving for feedback, suggestions, and encouragement. Thanks to Dr. Amanda Irwin Wilkins and "The Hare" writing workshop group for discussing and editing various figures and drafts of my Junior Papers and for being a wonderful group of creative, curious, and competent people who give excellent feedback and support and fed me dinner. Thank you to Prof. Adam C. Maloof who taught me LaTeXand for the past three years has provided an omnipresent voice in my head asking me if I was "changing the world" which has been both a source of inspiration and stress. Thanks to Dr. Chris Harig at the University of Arizona for providing some of the data files for my Fall Junior Paper. Thank you to Prof. Gabriel Vecchi for helpful insights into atmospheric and oceanic processes. Thank you to the numerous professors and graduate and undergraduate students in the Princeton Department of Geosciences for feedback, encouragement, and constructive criticism on various presentations of preliminary results. Thank you to all of my friends and family who read drafts of various independent work and provided helpful feedback. Lastly, an especially big thanks to all of the people who asked me, "What is your independent work about?" and then patiently listened while I struggled to articulate my project in a way that made any sense.

My Mom and Dad have always encouraged me to pursue my interests, and their support has opened up so many life-changing opportunities for me. Finally, thank you to Drew Brazer for making sure that I never missed room draw or course registration these past three years.

Contents

List of Figures

List of Tables

Introduction

Average global surface temperature is rising at an increasing rate — approximately 0.09° C per decade since 1880, and approximately 0.26° C per decade since 1979 (Hartmann et al., 2013) — with the past five years (2014–2018) being approximately 0.84° C warmer than the 1880–2018 average (NOAA, 2019). Earth's warming climate has contributed to significant melting of the Greenland ice sheet, and recent ice loss is estimated at -244 Gt per year (Harig & Simons, 2015, 2016). The Greenland Ice Sheet covers just over 1% of Earth's surface, and, if completely melted, would raise sea level by over 7 m (Vaughan et al., 2013). Global melting of ice sheets and glaciers accounts for almost half of recently observed rising sea levels, with Greenland alone contributing almost 25% of the 3 mm per year of sea level rise observed since 1993 (Nerem et al., 2018). Our broad goal is to understand the nature and cause of deviations from modeled rates of Greenland ice melt in order to better understand, predict, and communicate the changing conditions of the planet.

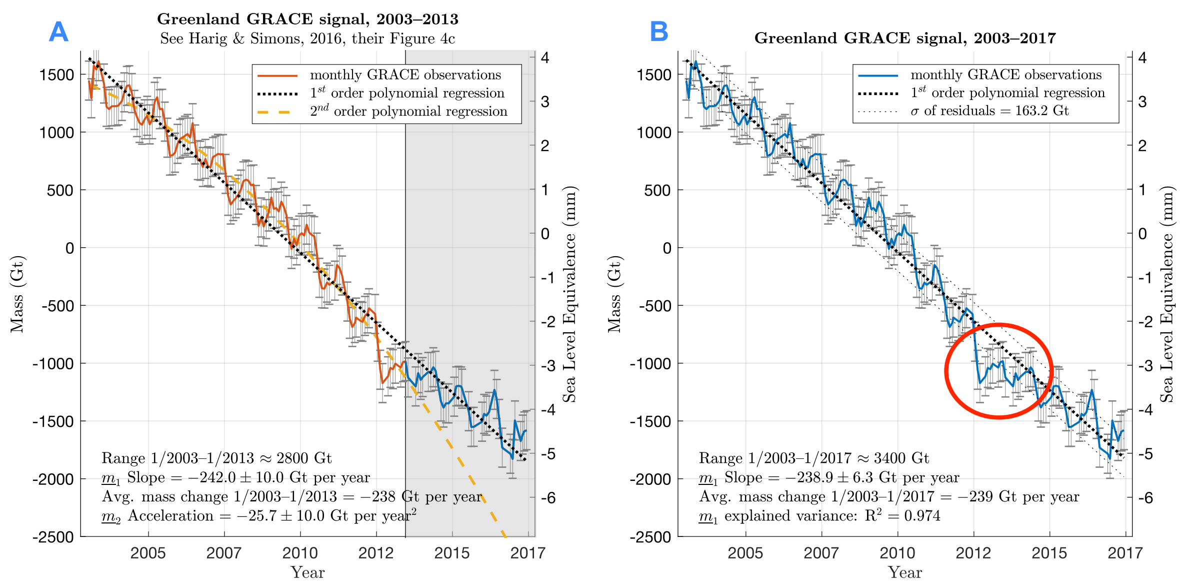

Figure 1: Total mass changes for Greenland over the complete GRACE record using equivalent methods to Harig & Simons (2016). Shown in **A** are the $\underline{m}_1$ (linear) and $\underline{m}_2$ (quadratic) models for 01/2003–06/2013, comparable to previous estimates of the mass trend (Harig & Simons, 2016). Note the significant departure of the extrapolated $\underline{m}_2$ model from the continuing signal. Shown in **B** is the $\underline{m}_1$ linear model for 01/2003–06/2017 with the standard of deviation of its residuals. Note that the $\underline{m}_1$ model does not significantly change after including the entire GRACE record. Error bars represent 2σ based on the combined variance of modeled Slepian coefficients f_α (see Harig & Simons (2016), as well as Getraer (2017, 2018)). This figure appeared in Getraer (2017, 2018), here with minor updates.

Ice loss on the Greenland Ice Sheet has been observed in gravitational measurements from NASA's Gravity Recovery and Climate Experiment (GRACE), satellite and airplane based altimetry, and energy balance models, finding acceleration of melt in the ice mass signal over most of the last two decades (Harig & Simons, 2016; Khan et al., 2015). Rates of ice loss increase by a combination of greater discharge from calving glacier termini at the edges of the ice-sheet and decreased surface mass-balance, the difference between seasonal snow accumulation and melting (Enderlin et al., 2014; Khan et al., 2015). Significant inter-annual variability and asynchronicity has been observed in the discharge rates of the Greenland Ice Sheet's major drainage basins, while surface mass-balance is comparatively more predictable (Enderlin et al., 2014; McMillan et al., 2016). Both contributions to ice loss accelerated between 2000–2012, combining for a total acceleration of ice mass estimated at nearly -30 Gt per year^2 over all of Greenland (Bevis et al., 2019; Enderlin et al., 2014; Velicogna, 2009).

A study by Harig & Simons (2016) modeling the mass of the Greenland Ice Sheet using GRACE data products showed deviations from the long-term accelerating trend, starting with a high level of melt in the summer of 2012, and followed by two summers of little melting in 2013 and 2014 (see Figure 1 A, comparable to Harig & Simons, 2016, their Figure 4). Our analysis of the complete GRACE data set (2002–2017) using identical methods showed a linear, not accelerating, trend of ice loss for the Greenland Ice Sheet, constraining the observed unexpected deviations to an unusually large melt summer of 2012 followed by a summer of unusually little melt in 2013 (see Figure 1 B).

The anomalous seasons of 2012–2013 have received attention in recent literature by studies attempting to understand how surface mass balance processes produce such inter-annual variability. Correlations have been found with climate indices such as the phase of the North Atlantic Oscillation (NAO) (Bevis et al., 2019; Getraer, 2017; McMillan et al., 2016), transient atmospheric transport of warm air and water vapor in so-called "atmospheric rivers" (Mattingly et al., 2018), and non-radiative energy flux enhanced by short-term cloud cover (Solomon et al., 2017).

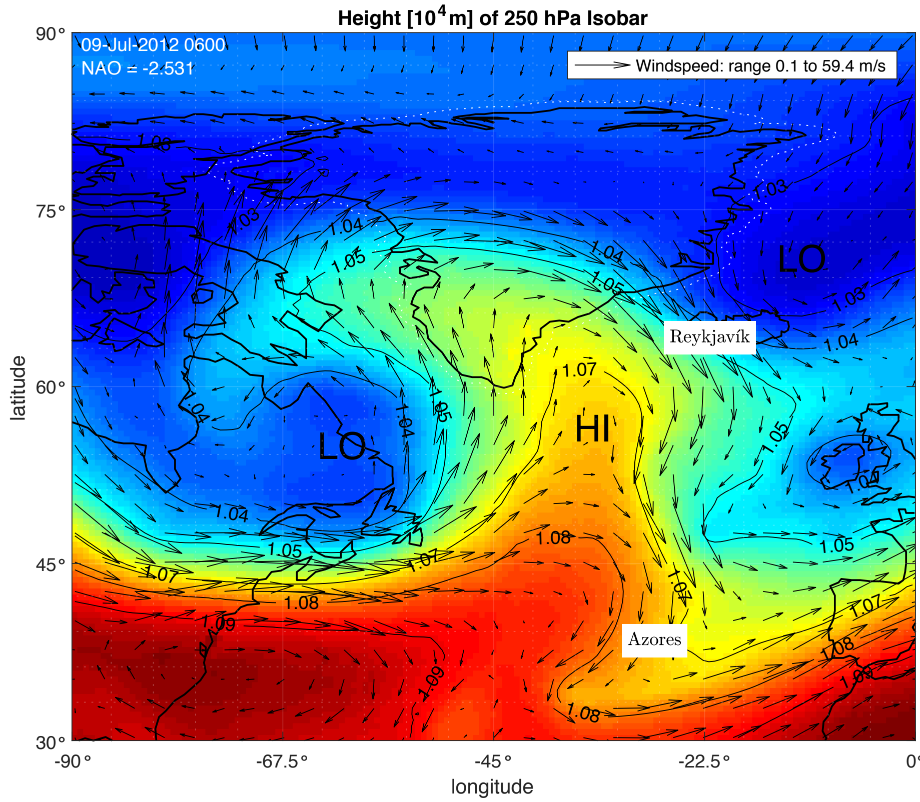

Figure 2: Example of atmospheric conditions at the 250 hPa isobar over the North Atlantic preceding record Greenland Ice Sheet surface melt, 07/09/2012 (from MERRA-2 reanalyzed data). Isobar height contours are labeled in 10^4 m, and wind vectors are shown by arrows. Note the location of the northern polar jet stream, dividing the low and high isobar heights around the 1.05×10^4 m contour. The temporary North Atlantic Rossby wave is labeled as the "HI" pressure anti-cyclone moving north towards southern Greenland, with a complementary "LO" pressure cyclone centered over Labrador. Note that the jet stream is deflected through the Labrador Sea and Baffin Bay, along the West Coast of Greenland. As a result of these conditions, the "LO" pressure over Reykjavík is pushed north, and the pressure difference between Reykjavík and Azores is lowered, resulting in an negative NAO index (top left).

Atmospheric Circulation Over the Greenland Ice Sheet

The atmospheric circulation affecting the Greenland Ice Sheet is broadly controlled by the position of the polar jet stream in the northern hemisphere (Hanna et al., 2013; Mattingly et al., 2018). The northern polar jet stream is a strong current of air moving generally eastward, dividing the warm, high pressure air of the temperate mid-latitudes and the cold, low pressure air of the Arctic. In the North Atlantic, the average position of the polar jet results in a low pressure Arctic system centered near Iceland, and a high pressure temperate system centered near the Azores. The strength of the polar jet stream moving air zonally across the North Atlantic is determined by the relative meridional pressure difference across the North Atlantic, and varies irregularly in what is called the North Atlantic Oscillation (NAO).

The NAO is often indexed for use in climate analyses by differencing the atmospheric pressure over the North Atlantic and a "loading pattern" of pressure determined by principal component analysis to capture the average meridional pattern (CPC, 2012; NCAR, 2019). A positive phase NAO index reflects a stronger meridional difference in pressure than usual, while negative values reflect a weaker meridional difference than usual (NCAR, 2019). The index is a unitless ratio normalized by the variance of atmospheric pressure from the loading pattern.

In studying melt events on the Greenland Ice Sheet, many studies have used an NAO index to relate melting conditions to atmospheric pressure patterns. Strong summer melt events often occur with a negative NAO index, suggesting that mechanisms which drive the NAO may have some kind of predictable implications for melting on Greenland (Bevis et al., 2019; Getraer, 2017; Hahn et al., 2018; Hanna et al., 2013; Mattingly et al., 2018; McMillan et al., 2016). More precisely, the use of the NAO index suggests that meridional pressure differences which drive westerly winds across the North Atlantic are a physical mechanism for strengthening melt conditions over Greenland — warm, moist air, and increased cloud cover (Bevis et al., 2019; Getraer, 2017; Hahn et al., 2018; Hanna et al., 2013; Mattingly et al., 2018; McMillan et al., 2016). This assumption, however, obscures the fact that melt events are often caused by southerly winds advecting atmospheric rivers of warm, moist air north, which is driven by a zonal difference in pressure (Hanna et al., 2013; Mattingly et al., 2018).

The polar jet does not maintain stable zonal flow, and regularly develops wiggles in which flow is diverted meridionally in large waves. During these events, known as a Rossby waves, temporary high-pressure systems push northward into the arctic accompanied by complementary low-pressure cyclones which develop on either side of the high-pressure block. The combined flow from these pressure systems advects warm air from the temperate mid-latitudes into the Arctic until the Rossby wave “breaks” and the jet stream return to its typical location.

Melt events on Greenland are generally driven by zonal differences in pressure resulting from Rossby wave systems with high pressure "blocking" over southern Greenland, which create atmospheric rivers advecting warm moist air over the ice sheet (Mattingly et al., 2018). In contrast, the NAO index measures against a meridional patterns of pressure, with the result that although melt events often correspond with a weaker NAO, a lower the NAO index does not strictly imply a greater melt event.

High pressure blocking over southern Greenland is often correlated with a negative NAO index, because the northern excursion of high pressure systems influences meridional pressure balance. However, despite their correlation, the two are fundamentally different atmospheric patterns which drive advection of air in different directions. In some recent studies, the Greenland Blocking Index (GBI) has been used, which is essentially the average pressure over Greenland. While this is more specific and more relevant than the NAO index, it still does not directly reflect the meridional advection which drives melt.

In this paper, I explore simple indices which directly compare zonal pressure differences which flow of warm air into the arctic over the Greenland Ice Sheet, and compare those results to the NAO and GBI indices.

Previous Results

Location of the 2012–2014

In my Spring 2018 JP, I explored the use of a 2-D wavelet basis to represent the GRACE gravimetric data over Greenland such that meaningfully contributing basis functions also contained information about spatial structure (see Figure 4).

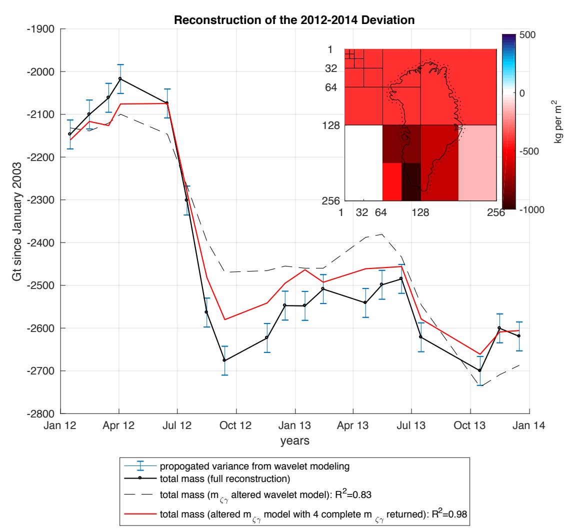

Figure 3: The 2012–2014 deviation in Greenland mass and the total from the reconstructed modeled wavelet coefficients. By adding in the real values of only four wavelet coefficients back into the modeled wavelet reconstruction we improve the variance explanation by 15%. These wavelets are shown inset, weighted by their values in September 2012, the extreme of the deviation, and are concentrated in southwestern Greenland. "$m_{\zeta\gamma}$" refers to a wavelet basis function "m" of index γ in level ζ. This Figure appeared in my Spring JP.

I developed a procedure for choosing the most important wavelet basis functions in order to extract the true fluctuation of the signal from the over-determined image calculated from the typical GRACE spherical harmonic basis. I then tested which wavelet basis function best captured the 2012–2013 deviation from the expected signal, finding the deviations to be concentrated in southwestern Greenland (see Figure 3).

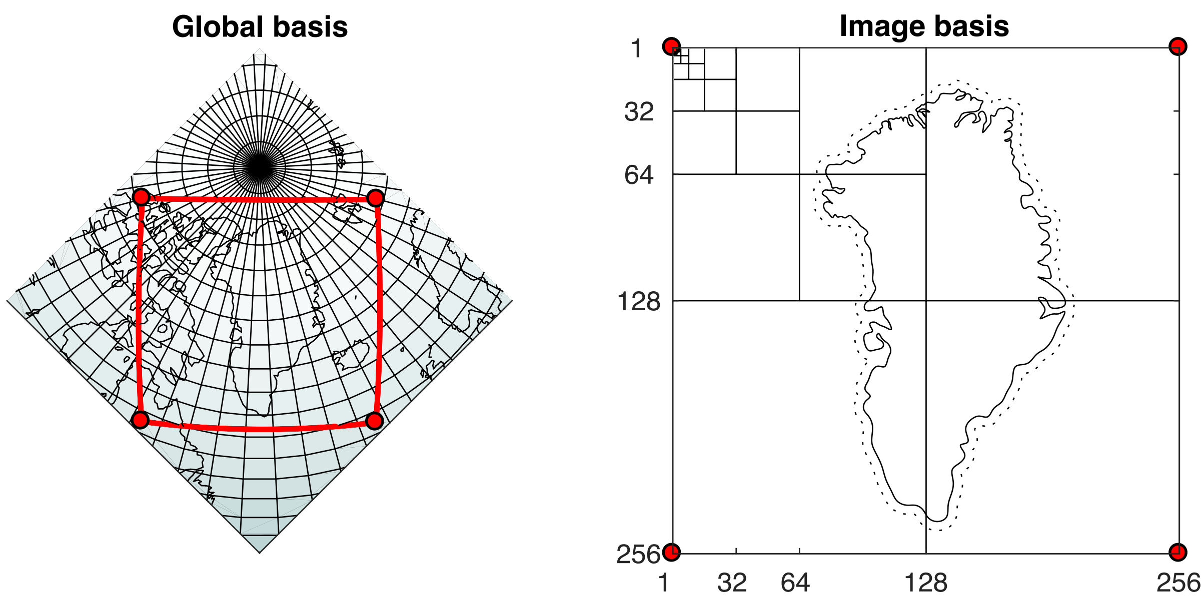

Figure 4: A grid is defined in the global basis on a face of the Cubed Sphere centered on Greenland, upon which the gravitational anomaly is evaluated from the GRACE spherical harmonic solutions. In the image basis the grid is cartesian with length 256. Grid lines in the image basis represent the diminishing spatial support of wavelets of different levels, from $\zeta = 8$ (the entire image) to $\zeta = 1$ (a unit grid cell). Note that in reality, each wavelet level has coverage over the entire image. The dotted line around Greenland is a coastal buffer of 0.5° as in Harig & Simons (2016). This Figure appeared in my Spring JP.

Data

Ice Mass Data

Observations of ice loss across large areas are measured remotely by satellites using several different methods, including weighing the mass by gravitational anomaly (such as NASA's GRACE and GRACE Follow-On missions), photographing surface area (such as NASA's Landsat and MODIS missions), and by measuring relative height of the ice with active laser altimetry (such as NASA's ICESat and ICESat-2 missions) (Khan et al., 2015).

Atmospheric Data

In addition to datasets which directly measure physical manifestations of ice sheet melting, there are complimentary datasets which capture some of the processes which control melting such as air temperature, humidity, and cloud cover. The primary atmospheric data used in this study are reanalysis products from the Modern-Era Retrospective analysis for Research and Applications, Version 2 (MERRA-2) (see Table 1 and Appendix A: Data and code sources).

Variable	**Temporal Resolution**	**Dataset**
2 Meter Air Temperature	daily	tavg1_2d_slv_Nx
	monthly	statM_2d_slv_Nx
500 hPa Air Temperature	daily	tavg1_2d_slv_Nx
2 Meter Air Specific Humidity	daily	tavg1_2d_slv_Nx
500 hPa Air Specific Humidity	daily	tavg1_2d_slv_Nx
Skin Surface Temperature	daily	tavg1_2d_slv_Nx
Total Cloud Area Fraction	daily	tavg1_2d_rad_Nx

Table 1: MERRA-2 data used in this study (see Appendix A: Data and code sources). Mean daily and monthly values were accessed on the default MERRA-2 $0.625°$ lon$\times$$0.5°$ lat grid with an original spatial resolution of approximately 50 km$\times$50 km(Bosilovich et al., 2016). Values are based on the GEOS climate models which combine direct observations into a globally continuous representation of the atmosphere, ocean, and surface interactions using a consistent set of of conservation assumptions (Bosilovich et al., 2016; Gelaro et al., 2017).

"Reanalysis" refers to a way of processing an ensemble of directly measured weather observations using a consistent set of rules that assume physical constraints on the ways in which different atmospheric variables interact temporally and spatially (Gelaro et al., 2017). These physical constraints are defined by a global climate model, which can both make forecasts of future developments of meteorological variables and output modeled solutions based on weather measurements directly observed at weather stations all over the world (Gelaro et al., 2017). Variable values for a given time and spatial location are calculated as a best fit of direct observations to the constraints of multiple different models which define processes such as radiation balances, physical movement, chemical interactions, precipitation, and so forth, or are inferred by the models' rules from variables which are directly measured (Bosilovich et al., 2016; Gelaro et al., 2017).

The data for this study come from NASA's Global Modeling and Assimilation Office's Goddard Earth Observing System (GEOS) climate models, and are publicly available in specific MERRA-2 data products through the NASA Goddard Earth Sciences Data Information Services Center (GES DISC) (see Appendix A: Data and code sources). MERRA-2 data are available in several different spatial and temporal formats for different variables. I use gridded daily averages for examining the connections between meteorological variables over the Greenland Ice Sheet, and gridded monthly averages for capturing the long-term development of Greenland's climate. Daily and monthly data are taken from collections of single-level, two-dimensional data which GES DISC provides in a few MERRA-2 datasets (see Table 1, Appendix A: Data and code sources).

Daily and monthly NAO climate index values are provided by the National Weather Service Climate Prediction Center, which calculates NAO index values from the 500 mb pressure level height over the spatial extent of 20–90° N (CPC, 2012). Pressure level heights are compared to a monthly loading pattern defined as the first principal component of a rotated principal component analysis on the 1950–2000 500 mb height time-series and values are normalized by monthly mean and standard of deviation for the 1950–2000 index time-series (see Appendix A: Data and code sources and CPC, 2012).

Lastly, Northern Hemisphere climate data are from the Goddard Institute for Space Studies Surface Temperature Analysis (GISTEMP v3) as a mean monthly Land-Ocean Temperature

Index (LOTI), which takes into account dampening of atmospheric temperature changes due to the heat capacity of ocean water (Hansen et al., 2010). The data used here are a monthly index of temperature anomalies from 1951–1980 time-series, which are available from 1880–present (see Appendix A: Data and code sources and Hansen et al., 2010).

Results

Over the 1980–2017 time period the Northern Hemisphere has been gradually warming, and averaging across the monthly LOTI anomaly with 10 year moving window reveals a quite linear trend of 0.24°C per decade (type 1 least-squares regression, with a variance reduction $R^2 = 0.987$), for a total increase of 0.89°C since 1980 (see Figure 5). Over the same time period, near surface temperature anomalies over the Greenland Ice Sheet had a significantly different pattern of increase, remaining static through the 1980's and more recently since the early 2000's, and increasing dramatically through the 1990's (Figure 5). Comparing the first 15 years (1980–1994) of the 1980–2017 time period to the last 15 years (2003–2017), the mean temperature rose 1.53 ± 0.42°C as illustrated in Figure 5 (two sample t-test found distributions of significantly different mean values, $p = 2.3\text{e}{-12}$; reported error represents the 95% confidence interval on the difference in mean values).

Rise in near surface air temperature across the Greenland Ice Sheet between 1980–2017 differed seasonally, with the greatest rise in temperature occurring in the Winter season (December, January, February) and the smallest rise in temperature occuring in the Summer season (June, July, August) (see Figure 6). The fitted linear trends were tested for significance against the hypothesis that a trend of the same magnitude could be generated from similar random data (normally distributed data of the same mean, standard of deviation, and number of points). p-values for the trends represent the percentage of trends of greater magnitude found in 10000 tests of similar random data. A similar method was used to calculate the confidence interval of these trends, by subtracting the linear fit, generating 10000 tests of similar random data, and finding the 90^{th} and 95^{th} percentile of slope magnitude amongst the random test data.

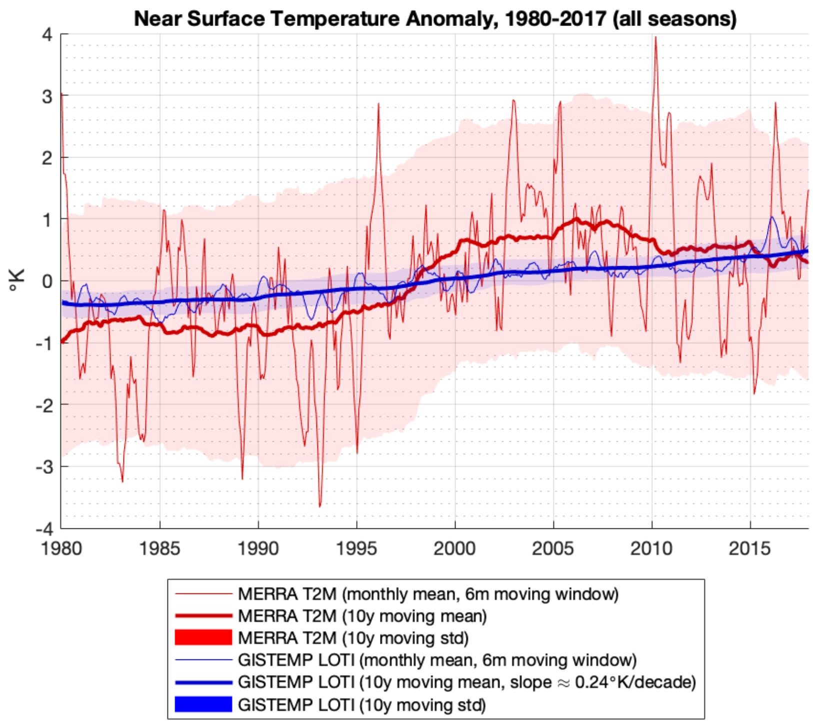

Figure 5: Mean monthly near surface temperature anomalies for the Northern Hemisphere (GISTEMP Land-Ocean Temperare Index, blue) and the Greenland Ice Sheet (MERRA-2 2m air temperature, red), 1980–2017. Data has been filtered using 6-month and 10-year moving windows for ease of interpretation, with the shaded area representing the spread of the data using the standard of deviation of the 10-year moving window. Note the more continuously linear increase in Northern Hemisphere temperature over the entire time-period compared to the non-linear jump in temperature over Greenland in the 1990's. Analyses of the unfiltered time-series show that: the Northern Hemisphere LOTI is increasing at 0.24°C per decade ($R^2 = 0.987$); near-surface air temperature increased 1.53 ± 0.42°C between the years 1980–1994 and 2003–2017.

For the seasonal near surface air temperature trends between 1980–2017, all were found to be significant at at least the $p < 0.05$ threshold compared to the 10000 tests of similar random data (see Table 2). The difference in trend between Winter and Summer months is significant in the random simulations, with the best fit trend for each falling outside of the 90% confidence interval of the other (see Table 2).

Despite the overall rise in temperature since the 1980's, near surface air temperature across the Greenland Ice Sheet was not increasing over the GRACE record (2003–2017) (Figure 6). In fact, mean 2m air temperature anomaly over the ice sheet drifted cooler in every season

Season	Trend [°C/decade]	95% conf. int.	90% conf. int.	p-value
1980–2017				
Winter (DJF)	+0.80	±0.46	±0.38	0.0015
Spring (MAM)	+0.46	±0.36	±0.30	0.0163
Summer (JJA)	+0.35	±0.17	±0.15	0.0002
Fall (SON)	+0.48	±0.29	±0.25	0.0021
2003–2017				
Winter (DJF)	−0.47	±1.12	±0.93	0.413
Spring (MAM)	−0.96	±1.11	±0.94	0.105
Summer (JJA)	−0.72	±1.13	±0.94	0.217
Fall (SON)	−0.02	±1.13	±0.94	0.971

Table 2: Seasonal trends in MERRA-2 2m air temperature calculated on mean monthly data across the Greenland Ice Sheet for the time period 1980–2017 and 2003–2017, shown in Figure 6. The trend is the type 1 least squares regression slope of the mean monthly data, and confidence intervals are the results of synthetic data tests analyzing the residuals of the data and the trend line. p-values represent the chances of finding a trend slope of equal or greater magnitude in a random sampling of a "similar" normal distribution. For 1980–2017, all seasons have trend magnitudes that are significantly different from a random sampling of a "similar" normal distribution at the $p < 0.05$ threshold; Winter and Summer seasonal trends are significantly different from each other at the 90% confidence interval; Fall and Spring trends are not significantly different from Summer, and are not well differentiated from Winter. For 2003–2017, Winter and Fall trends are well within expected fits for similar random data, and while the Spring and Summer trends are more unusual, those negative trends are also not significantly differentiable from similar random data in p-value or confidence interval.

Discussion

Greenland is melting, is it warming?

The melting of the Greenland Ice Sheet is strongly connected to warming temperatures in much of the literature, and the significant repercussions of various short-term warming scenarios on the evolution of ice sheet melting are of great importance to predicting sea-level rise over the next century (Hahn et al., 2018; Pattyn et al., 2018; Rückamp et al., 2018). To best understand the relationship between warming temperatures and Greenland melt, some caution must be used in drawing a direct line between increasing mean global surface temperatures and increases of melt on the Greenland ice sheet.

Between the late 1990's and 2012, an apparent pause in the rise of mean global temperatures coincided with the strongest acceleration in Greenland ice sheet mass loss of the last century (Bevis et al., 2018; Kosaka & Xie, 2013; Van Angelen et al., 2014). The "hiatus" observed in global warming over the first decade of the 21st century has been correlated with natural climate variability such as the El Niño/Southern Oscillation (ENSO), with heat being stored in cooler La Niña ocean waters (Kosaka & Xie, 2013). Between 2012 and 2017, mean global temperatures resumed a strong upwards trend driven by a negative to positive shift in ENSO phase (see Fig. 8).

Over the same period, mean Greenland Ice Sheet near-surface temperature did not rise significantly, and in fact was decreasing slightly across almost the entire ice sheet between 2003 and 2017 (see Figs. 8 & 9, and Hearty et al., 2018; Reeves Eyre & Zeng, 2017; Westergaard-Nielsen et al., 2018). Temperatures over Greenland are expected to continue to rise with global temperatures into the future, but have not done so significantly since the 1990's (Reeves Eyre & Zeng, 2017).

In interpreting the record of Greenland Ice Sheet mass wasting, it is important to note that the linear trend observed over the entire 2003–2017 GRACE record need not be driven by changing climate over that time period. Warming mean temperatures over Greenland in the 1990's drove the ice sheet into the linear decline we have seen in the GRACE record, with an approximately constant amount of summer loss each year (Getraer, 2017). Over that time period, anomalous years and accelerations in melt are likely due to variability in weather patterns across Greenland and the North Atlantic, and not regional or global warming (Bevis et al., 2018; Hahn et al., 2018).

NAO Correlation with Melt

Often times when comparing the NAO to Greenland melt, monthly or seasonal means are used to correlate with melt events that occur over time scales of a few days (see, for example, Bevis et al., 2018; Mattingly et al., 2018; Van Angelen et al., 2014). These averaged NAO index values are used despite the fact that daily and sub-daily solutions are readily available for the NAO index, and despite the fact that the physical atmospheric drivers of melting (such as temperature, cloud cover, etc.) are changing on a daily, not monthly, basis, and are interacting directly with atmospheric pressure (for example, Mattingly et al., 2018).

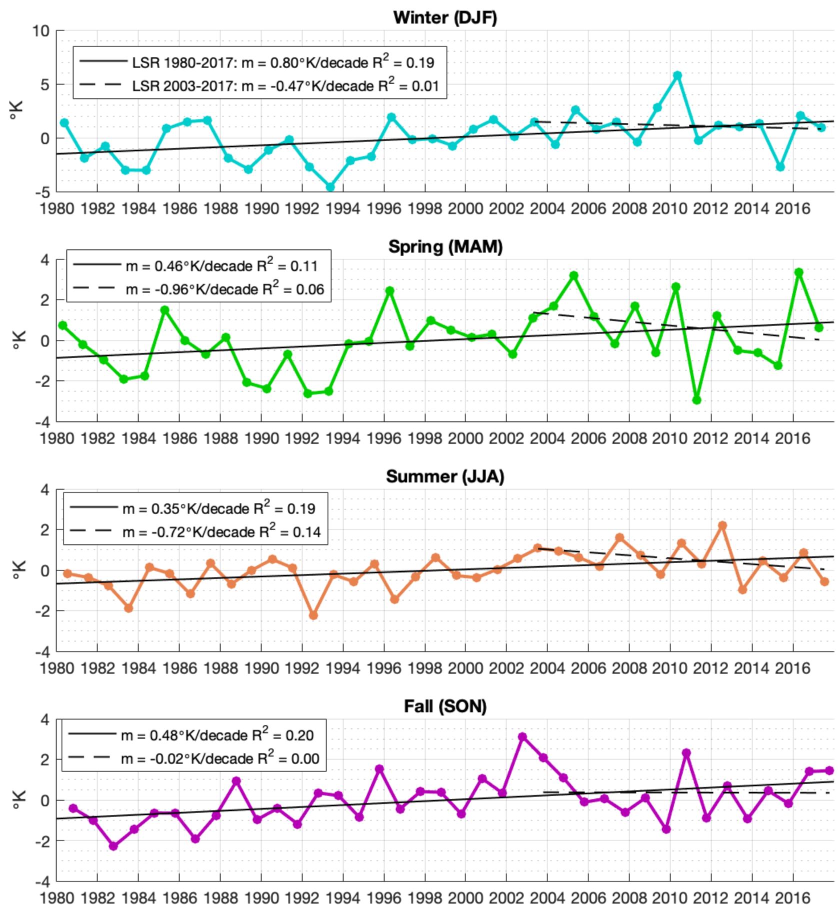

Figure 6: Seasonal trends in MERRA-2 2m air temperature across the Greenland Ice Sheet for 1980–2017. Plotted points are the seasonal mean for each year, and are fit with a type-1 least squares regression for the full time period (solid) and the GRACE time period (dashes). Note that between 1980–2017 Winter temperatures warmed more than summer temperatures, while during the GRACE time period (2003–2017) Summer temperatures dropped more than Winter temperatures. Table 2 contains an analysis of the significance of each trend and its confidence interval, showing that the seasonal trends in mean monthly temperature over the full time period are significant, while the seasonal trends over the GRACE period are not significantly differentiable (in both *p*-value and confidence interval) from trends in random data drawn randomly from a similar normal distribution.

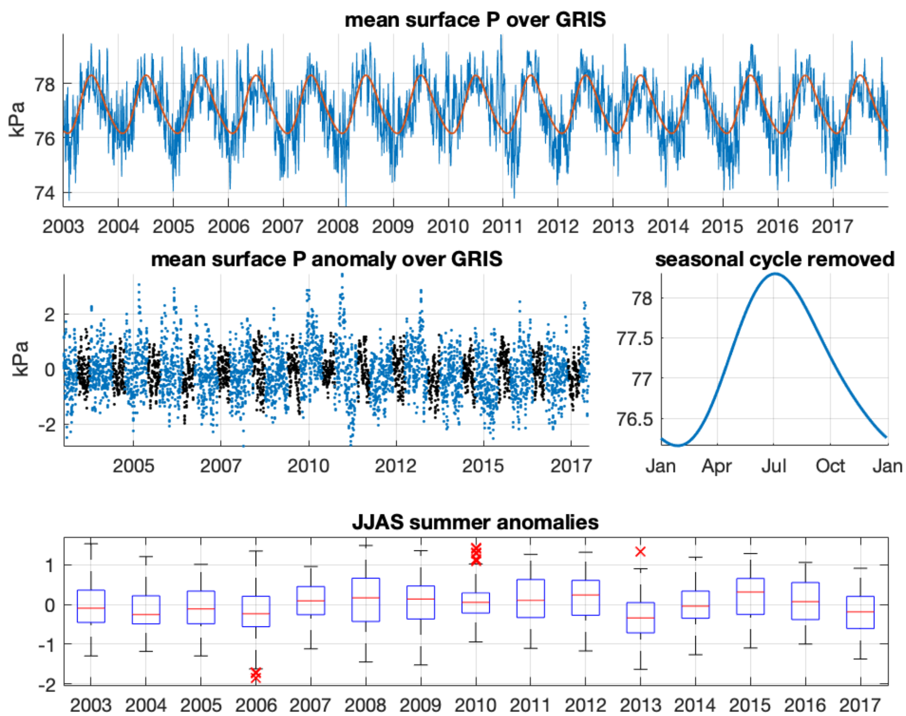
mean surface P over GRIS
kPa
78
76
74
2003 2004 2005 2006 2007 2008 2009 2010 2011 2012 2013 2014 2015 2016 2017
mean surface P anomaly over GRIS
kPa
2
0
-2
2005 2007 2010 2012 2015 2017
seasonal cycle removed
78
77.5
77
76.5
Jan Apr Jul Oct Jan
JJAS summer anomalies
1
0
-1
-2
2003 2004 2005 2006 2007 2008 2009 2010 2011 2012 2013 2014 2015 2016 2017

Figure 7

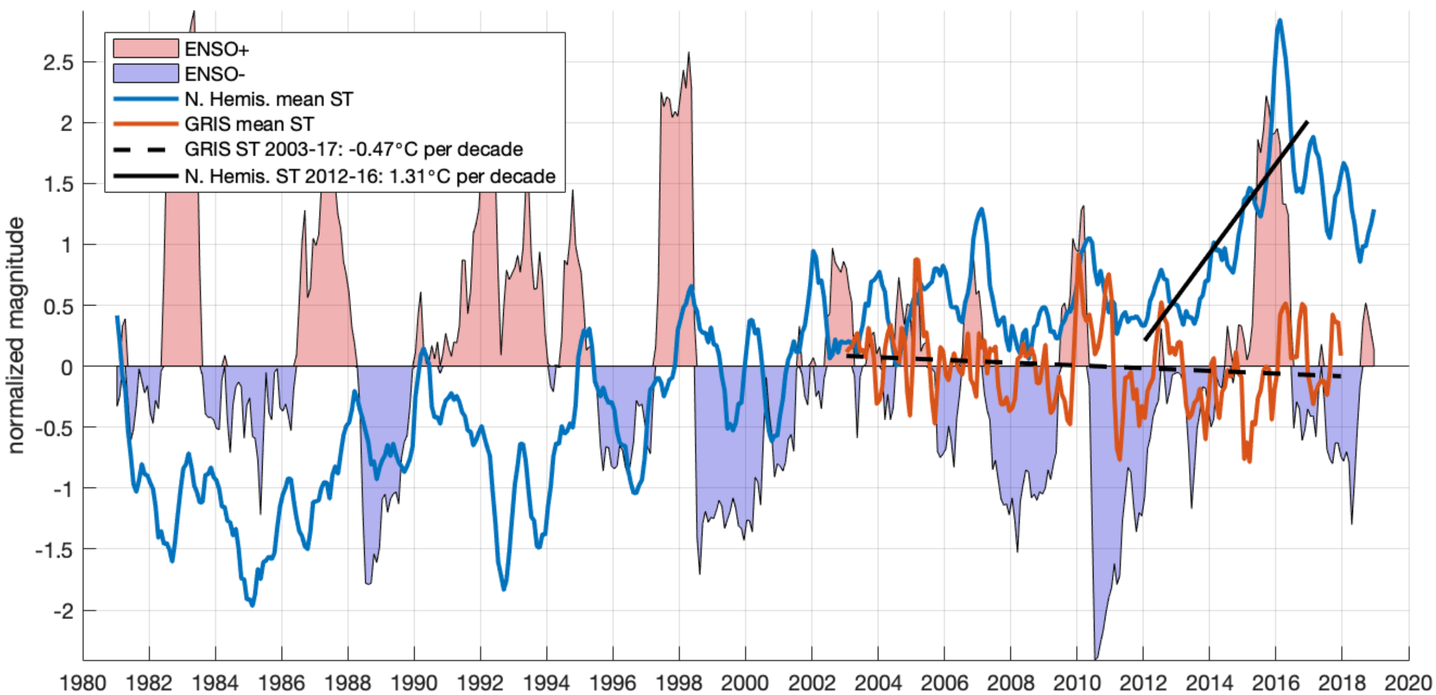
ENSO+
ENSO-
N. Hemis. mean ST
GRIS mean ST
GRIS ST 2003-17: -0.47°C per decade
N. Hemis. ST 2012-16: 1.31°C per decade
normalized magnitude
2.5
2
1.5
1
0.5
0
-0.5
-1
-1.5
-2
1980
1982
1984
1986
1988
1990
1992
1994
1996
1998
2000
2002
2004
2006
2008
2010
2012
2014
2016
2018
2020

Figure 8

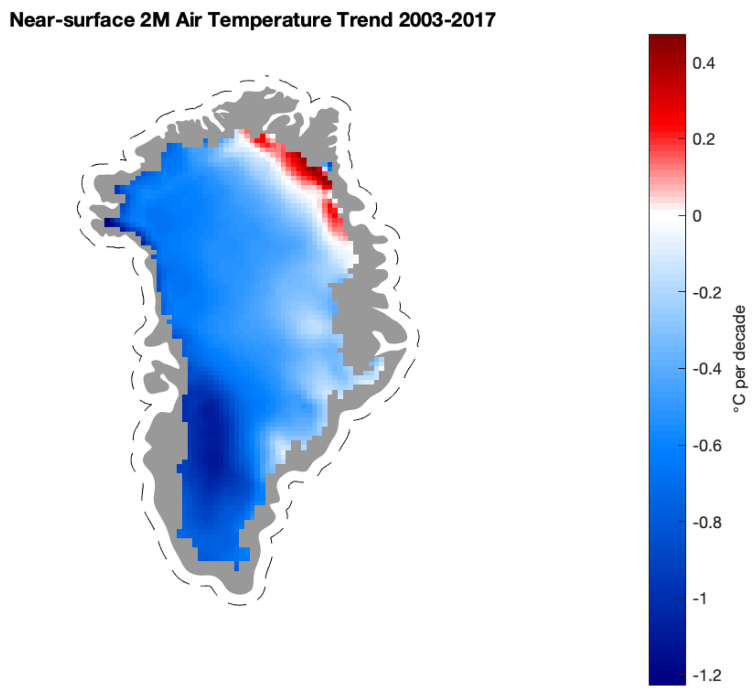
Near-surface 2M Air Temperature Trend 2003-2017
0.4
0.2
0
-0.2
-0.4
-0.6
-0.8
-1
-1.2
°C per decade

Figure 9

Appendix A: Data and code sources

RL05 spherical harmonic coefficients for the time-variant geopotential field from the Center for Space Research data processing center at The University of Texas at Austin are available at:

`ftp://podaac.jpl.nasa.gov/allData/grace/L2/CSR/RL05`

Coefficients describing Earth's center of mass (spherical harmonic degree 1, from Swenson et al., 2008) are available at:

`ftp://podaac-ftp.jpl.nasa.gov/GeodeticsGravity/tellus/L2/degree_1/`

Coefficients describing Earth's oblateness (spherical harmonic degree 2, order 0, from Cheng et al., 2013) are available at:

`ftp://ftp.csr.utexas.edu/pub/slr/degree_2/`

Index values for the North Atlantic Oscillation are calculated by the National Weather Service Climate Prediction Center (see CPC, 2012), with normalized monthly average values since January 1950 available at:

`ftp://ftp.cpc.ncep.noaa.gov/wd52dg/data/indices/nao_index.tim`

Normalized daily values since January 1950 are available at:

`ftp://ftp.cpc.ncep.noaa.gov/cwlinks/norm.daily.nao.index.b500101.current.ascii`

MERRA-2 atmospheric reanalysis data are calculated by the NASA Global Modeling and Assimilation Office (GMAO) as part of the activities of NASA's Science Mission Directorate, and are archived and distributed by the Goddard Earth Sciences Data and Information Services Center (GES-DISC). All data was accessed between September 2018 and April 2019.

A graphical user interface for generating data download links for specific subsets of variables, space, and time is available at: `https://disc.gsfc.nasa.gov`

Data used in this study can be directly accessed at the following addresses:

`https://goldsmr4.gesdisc.eosdis.nasa.gov/data/MERRA2_MONTHLY/M2SMNXSLV.5.12.4/`

`https://goldsmr4.gesdisc.eosdis.nasa.gov/data/MERRA2/M2T1NXSLV.5.12.4/`

`https://goldsmr4.gesdisc.eosdis.nasa.gov/data/MERRA2/M2T1NXRAD.5.12.4/`

Northern Hemisphere Land-Ocean Temperature Index anomalies from NASA's Goddard Institute for Space Studies Surface Temperature Analysis (GISTEMP v3, see Hansen et al., 2010) were accessed in March 2019 and are available at:

`https://data.giss.nasa.gov/gistemp/tabledata_v3/NH.Ts+dSST.csv`

MATLAB code for the expansion and manipulation of spherical harmonic eigenfunctions into Slepian bases and manipulation of GRACE files is borrowed and adapted from:

`https://github.com/csdms-contrib/`

MATLAB code developed for this project, including functions for executing the wavelet analysis and scripts for generating figures, can be accessed at:

`https://github.com/bgetraer/slepian_bgetraer/`

References

Bevis, M., Harig, C., Khan, S. A., Brown, A., Simons, F. J., Willis, M., Fettweis, X., van den Broeke, M. R., Madsen, F. B., Kendrick, E., Caccamise II, D. J., van Dam, T., Knudsen, P., & Nylen, T., 2018. Accelerating changes in ice mass within Greenland, and the ice sheet's sensitivity to atmospheric forcing, *in submission to Proc. Natl. Acad. Sc.*.

Bevis, M., Harig, C., Khan, S. A., Brown, A., Simons, F. J., Willis, M., Fettweis, X., van den Broeke, M. R., Madsen, F. B., Kendrick, E., Caccamise, D. J., van Dam, T., Knudsen, P., & Nylen, T., 2019. Accelerating changes in ice mass within Greenland, and the ice sheet's sensitivity to atmospheric forcing, *Proceedings of the National Academy of Sciences*, **116**(6), 1934–1939, doi: 10.1073/pnas.1806562116.

Bosilovich, M. G., Lucchesi, R., & Suarez, M., 2016. MERRA-2: File Specification, *GMAO Office*, **Note No. 9 (Version 1.1), available from `http://gmao.gsfc.nasa.gov/pubs/office_notes`**.

Cheng, M., Tapley, B. D., & Ries, J. C., 2013. Deceleration in the Earth's oblateness, *Journal of Geophysical Research: Solid Earth*, **118**(2), 740–747, doi: 10.1002/jgrb.50058.

CPC, 2012. Northern Hemisphere Teleconnection Patterns, *National Weather Service Climate Prediction Center (Eds)*, **published online, last modified January 2012 at `https://www.cpc.ncep.noaa.gov/data/teledoc/telecontents.shtml`**.

Enderlin, E. M., Howat, I. M., Jeong, S., Noh, M.-J., van Angelen, J. H., & van den Broeke, M. R., 2014. An improved mass budget for the Greenland ice sheet, *Geophysical Research Letters*, **41**(3), 866–872 doi 10.1002/2013GL059010.

Gelaro, R., McCarty, W., SuÃ¡rez, M. J., Todling, R., Molod, A., Takacs, L., Randles, C. A., Darmenov, A., Bosilovich, M. G., Reichle, R., Wargan, K., Coy, L., Cullather, R., Draper, C., Akella, S., Buchard, V., Conaty, A., da Silva, A. M., Gu, W., Kim, G.-K., Koster, R., Lucchesi, R., Merkova, D., Nielsen, J. E., Partyka, G., Pawson, S., Putman, W., Rienecker, M., Schubert, S. D., Sienkiewicz, M., & Zhao, B., 2017. The Modern-Era Retrospective Analysis for Research and Applications, Version 2 (MERRA-

2), *Journal of Climate*, **30**(14), 5419–5454, doi: 10.1175/JCLI–D–16–0758.1.

Getraer, B., 2017. Resolving and Contextualizing the Signal of Greenland Ice Loss 2014–2017, *Princeton Department of Geosciences*, **Fall Junior Paper, unpublished**.

Getraer, B., 2018. Regional Forcing of Greenland Ice Loss 2002–2017, *Princeton Department of Geosciences*, **Spring Junior Paper, unpublished**.

Hahn, L., Ummenhofer, C. C., & Kwon, Y.-O., 2018. North Atlantic Natural Variability Modulates Emergence of Widespread Greenland Melt in a Warming Climate, *Geophysical Research Letters*, **45**(17), 9171–9178.

Hanna, E., Fettweis, X., Mernild, S. H., Cappelen, J., Ribergaard, M. H., Shuman, C. A., Steffen, K., Wood, L., & Mote, T. L., 2013. Atmospheric and oceanic climate forcing of the exceptional Greenland ice sheet surface melt in summer 2012, *International Journal of Climatology*, **34**(4), 1022–1037.

Hansen, J., Ruedy, R., Sato, M., & Lo, K., 2010. Global Surface Temperature Change, *Reviews of Geophysics*, **48, RG4004**, 1–29, doi:10.1029/2010RG000345.

Harig, C. & Simons, F. J., 2015. Accelerated West Antarctic ice mass loss continues to outpace East Antarctic gains, *Earth Planet. Sci. Lett.*, **415**, 134–141, doi: 10.1016/j.epsl.2015.01.029.

Harig, C. & Simons, F. J., 2016. Ice mass loss in Greenland, the Gulf of Alaska, and the Canadian Archipelago: Seasonal cycles and decadal trends, *Geophysical Research Letters*, **43**(7), 3150–3159, doi: 10.1002/2016GL067759.

Hartmann, D., Tank, A. K., Rusticucci, M., Alexander, L., Brönnimann, S., Charabi, Y., Dentener, F., Dlugokencky, E., Easterling, D., Kaplan, A., Soden, B., Thorne, P., Wild, M., & Zhai, P., 2013. *Climate Change 2013: The Physical Science Basis. Contribution of Working Group I Contribution to the Fifth Assessment Report of the Intergovernmental Panel on Climate Change*, chap. Observations: Atmosphere and Surface, p. doi: 10.1017/CBO9781107415324, Cambridge Univ. Press.

Hearty, T. J., Lee, J. N., Wu, D. L., Cullather, R., Blaisdell, J. M., Susskind, J., & Nowicki, S. M. J., 2018. Intercomparison of Surface Temperatures from AIRS, MERRA, and MERRA-2 with NOAA and GC-Net Weather Stations at Summit, Greenland, *Journal of Applied Meteorology and Climatology*, **57**(5), 1231–1245.

Khan, S. A., Aschwanden, A., Bjørk, A. A., Wahr, J., Kjeldsen, K. K., & Kjær, K. H., 2015. Greenland ice sheet mass balance: a review, *Reports on Progress in Physics*, **78**(4), 046801.

Kosaka, Y. & Xie, S.-P., 2013. Recent global-warming hiatus tied to equatorial Pacific surface cooling, *Nature*, **501**(7467), 403.

Mattingly, K., Mote, T., & Fettweis, X., 2018. Atmospheric River Impacts on Greenland Ice Sheet Surface Mass Balance, *Journal of Geophysical Research: Atmospheres*, **123**, 8538–8560, doi: 10.1029/2018JD028714.

McMillan, M., Leeson, A., Shepherd, A., Briggs, K., Armitage, T. W., Hogg, A., Munneke, P. K., van den Broeke, M., Noël, B., van de Berg, W. J., Ligtenberg, S., Horwath, M., Groh, A., Muir, A., & Gilbert, L., 2016. A high-resolution record of Greenland mass balance, *Geophysical Research Letters*, **43**(13), 7002–7010, doi: 10.1002/2016GL069666.

NCAR, 2019. The Climate Data Guide: Hurrell North Atlantic Oscillation (NAO) Index (PC-based), *National Center for Atmospheric Research Staff (Eds)*, **published online, last modified January 2019 at `https://climatedataguide.ucar.edu/climate-data/hurrell-north-atlantic-oscillation-nao-index-pc-based`**.

Nerem, R. S., Beckley, B. D., Fasullo, J. T., Hamlington, B. D., Masters, D., & Mitchum, G. T., 2018. Climate-change–driven accelerated sea-level rise detected in the altimeter era, *Proceedings of the National Academy of Sciences*, **115**(9), 2022–2025, doi: 10.1073/pnas.1717312115.

NOAA, 2019. State of the Climate: Global Climate Report for Annual 2018, *National Centers for Environmental Information*, **published online, January 2019 at `https://www.ncdc.noaa.gov/sotc/global/201813`**.

Pattyn, F., Ritz, C., Hanna, E., Asay-Davis, X., DeConto, R., Durand, G., Favier, L., Fettweis, X., Goelzer, H., Golledge, N. R., et al., 2018. The Greenland and Antarctic Ice Sheets Under 1.5Â° C Global Warming, *Nature Climate Change*, p. 1.

Reeves Eyre, J. & Zeng, X., 2017. Evaluation of Greenland near surface air temperature datasets, *The Cryosphere*, **11**(4), 1591–1605.

Rückamp, M., Greve, R., & Humbert, A., 2018. Comparative Simulations of the Evolution of the Greenland Ice Sheet Under Simplified Paris Agreement Scenarios with the Models SICOPOLIS and ISSM, *Polar Science*.

Solomon, A., Shupe, M. D., & Miller, N. B., 2017. Cloud-Atmospheric Boundary Layer-Surface Interactions on the Greenland Ice Sheet during the July 2012 Extreme Melt Event, *Journal of Climate*, **30**(9), 3237–3252.

Swenson, S., Chambers, D., & Wahr, J., 2008. Estimating geocenter variations from a combination of GRACE and ocean model output, *Journal of Geophysical Research: Solid Earth*, **113**(B8), doi: 10.1029/2007JB005338.

Van Angelen, J., Van den Broeke, M., Wouters, B., & Lenaerts, J., 2014. Contemporary (1960–2012) evolution of the climate and surface mass balance of the Greenland ice sheet, *Surveys in Geophysics*, **35**(5), 1155–1174.

Vaughan, D., Comiso, J., Allison, I., Carrasco, J., Kaser, G., Kwok, R., Mote, P., Murray, T., Paul, F., Ren, J., Rignot, E., Solomina, O., Steffen, K., & Zhang, T., 2013. *Climate Change 2013: The Physical Science Basis. Contribution of Working Group I Contribution to the Fifth Assessment Report*, chap. Observations: Cryosphere, p. doi: 10.1017/CBO9781107415324, Cambridge Univ. Press.

Velicogna, I., 2009. Increasing rates of ice mass loss from the Greenland and Antarctic ice sheets revealed by GRACE, *Geophysical Research Letters*, **36**(19), doi 10.1029/2009GL040222, L19503.

Westergaard-Nielsen, A., Karami, M., Hansen, B. U., Westermann, S., & Elberling, B., 2018. Contrasting temperature trends across the ice-free part of Greenland, *Scientific reports*, **8**(1), 1586.